Journal of Theoretical Biology 414 (2017) 137–146

Contents lists available at ScienceDirect

Journal of Theoretical Biology

journal homepage: www.elsevier.com/locate/yjtbi

Limited by sensing - A minimal stochastic model of the lag-phase during diauxic growth

Dominique Chu

School of Computing, University of Kent, CT2 7NF Canterbury, UK

ARTICLE INFO

Keywords:
Diauxic growth
Brownian computers
Stochastic systems
Biological sensors

ABSTRACT

Many microbes when grown on a mixture of two carbon sources utilise first and exclusively the preferred sugar, before switching to the less preferred carbon source. This results in two distinct exponential growth phases, often interrupted by a lag-phase of reduced growth termed the *lag-phase*. While the lag-phase appears to be an evolved feature, it is not clear what drives its evolution, as it comes with a substantial up-front fitness penalty due to lost growth. In this article a minimal mathematical model based on a master-equation approach is proposed. This model can explain many empirically observed phenomena. It suggests that the lag-phase can be understood as a manifestation of the trade-off between switching speed and switching efficiency. Moreover, the model predicts heterogeneity of the population during the lag-phase. Finally, it is shown that the switch from one carbon source to another one is a sensing problem and the lag-phase is a manifestation of known fundamental limitations of biological sensors.

1. Introduction

Diauxic growth is the phenomenon whereby a population of microbes, when presented with two carbon sources, exhibits bi-phasic exponential growth intermitted by a *lag phase* of minimal growth. Originally, the phenomenon was described by Monod (1949) demonstrating diauxie with glucose and lactose in *E.coli*. In his experiments Monod showed that the population first grows exponentially on glucose until all glucose is exhausted, then enters the lag-phase of no growth before resuming exponential growth on lactose. The duration of the lag-phase can be substantial (order of magnitude of a generation time).

Diauxic growth and the network that controls it has since been subject to intense experimental (Stülke and Hillen, 1999; Brückner and Titgemeyer, 2002; Boulineau et al., 2013; Boianelli et al., 2012; Inada et al., 1996; Kompala et al., 1986; New et al., 2014) and theoretical (Boianelli et al., 2012; Narang, 2006; Narang and Pilyugin, 2007; Kremling et al., 2009) investigation. There are two main mechanisms responsible for two phase growth in bacteria, both of which depend on the *phosphotransferase* (PTS) system (Deutscher, 2008): (*i* Regulation of metabolic genes via global transcription regulators, especially cAMP. (*ii*) Direct uptake mediated inducer exclusion. In *E.coli* the levels of dephospho $EIIA^{glc}$ increase during glucose uptake. $EIIA^{glc}$ inactivates the uptake of the secondary sugars (i.e. lactose) and in this way prevents the induction of the relevant uptake system.

Diauxic growth is generally believed to be an adaptation to optimise growth in multi-nutrient environments. Indeed, there is a clear argument that sequential uptake is beneficial in that it maximises the share of the higher quality nutrient for the lineage. Yet, by the same token one would have to conclude that a lag-phase is detrimental in that it is not at all conducive to the overall goal of maximising growth. Instead, it entails a substantial episodic fitness penalty as it allows hypothetical competitors that continue growth to monopolise carbon sources, at least temporarily.

Experimental evolution experiments (New et al., 2014) demonstrate that there is an optimal duration. The optimum depends on the environmental conditions, in particular the frequency with which carbon sources change. This shows that the duration of the lag-phase is under evolutionary control and not just an unavoidable design feature of cells. An implication of this is that the episodic fitness cost of the lag-phase is balanced by some long-term benefit. The experiments described in (New et al., 2014) suggest that the evolution of the lag-phase is driven by a general trade-off between the ability of the cell to switch rapidly between metabolic states and maximum steady-state growth rates on a particular nutrient. Such a trade-off between the ability to grow fast and adapt well is known empirically (Kotte et al., 2014), but its ultimate mechanistic origin remains unclear.

In this contribution we will propose that this trade-off can be due to fundamental physical limitations of biological sensors. Diauxic growth is not normally thought of as a problem of sensing. Yet, clearly the accurate detection of the external conditions is a *sine qua non* for the diauxic shift. The decision of an individual cell to activate the secondary pathway depends on it having detected (*i* that the secondary nutrient is present and (*ii*) that the primary nutrient has depleted sufficiently. Any delay in the sensing of external conditions necessarily puts a lower bound on the lag-phase.

It is now well established that the ability of biological cells to sense

http://dx.doi.org/10.1016/j.jtbi.2016.10.019
Received 30 December 2015; Received in revised form 3 October 2016; Accepted 28 October 2016
Available online 04 November 2016

is fundamentally limited by the stochastic nature of the biochemical detectors (Berg and Purcell, 1977; Bialek and Setayeshgar, 2005; Barato and Seifert, 2015). Reducing the sensing error is only possible at the expense of higher resource usage, either through an increase of the number of sensing particles or the maintenance of a free energy gradient (Govern and ten Wolde, 2014, 2014). This leads to the trade-off between fast adaptation and fast growth which fundamentally is a trade-off between the long-term costs of maintaining better sensors (necessary for fast switching) and the episodic fitness penalty during the diauxic shift.

This explanatory *ansatz* is also suggested by some recent empirical studies of diauxie. Single-cell observations of *E.coli* diauxie reveal significant intra-population heterogeneity (Boulineau et al., 2013) and phenotypic variability of metabolic states during the diauxic shift (Kotte et al., 2014). These studies indicate that during the lag-phase a small proportion of cells continue to grow, and many cells never switch to the secondary carbon source, but instead enter a dormant state (Solopova et al., 2014).

For *Saccharomyces cerevisiae* (Wang et al., 2015) and (Venturelli et al., 2015) report detailed measurements of diauxie. Importantly, they found that universally the population begins to switch to the secondary nutrient *before* the primary carbon source is exhausted (Wang et al., 2015). The timing of this switch to the secondary nutrient determines the length of the lag phase. Cell lines that switch later tend to have longer lag-phases (Wang et al., 2015). Finally, at low concentrations of the secondary nutrient the system is able to display "bistability" (Venturelli et al., 2015), i.e. co-existence of two sub-populations characterised by an activated and suppressed secondary metabolism respectively. A priori, it is not clear whether or not these observations are fundamentally connected to diauxic growth, or whether they are incidental, due to some other species specific features of the regulatory networks. We will argue here, that they can be understood as necessary consequences of the limitations of biological sensors. The same limitations can be understood as giving rise to the lag-phase itself.

Here we describe a minimal model of inducer exclusion based on the bacterial PTS system. We show that this model is consistent with the experimentally observed properties of diauxic growth, i.e. it predicts bistability, pre-mature switching to the secondary nutrient and population heterogeneity. More significantly, this minimal model traces the origin of the lag-phase and the growth/switching trade-off to the limitations of biological sensors. It predicts that the stochastic limitation of the sensor manifests itself as an area of uncertainty where the cell is unable to determine whether or not the primary nutrient has fallen below a certain threshold concentration; this makes switching *inaccurate*. This inaccuracy is a source of phenotypic variation and may explain the observed population heterogeneity. We also show analytically (for a simplified model) and numerically (for a more complicated version) that fast switching (from the primary to the secondary nutrient), and hence a short lag-phase, is only possible if the threshold number of permeases is high, i.e. there is a trade-off between the speed of switching and the efficiency of switching. This recapitulates the relationship found empirically by Wang et al. (2015). It really means that cells that for a cell to be able to switch fast, it needs to start to switch well before glucose is depleted from the environment. Finally, the model also predicts that fast switching, and hence a short lag-phase depends on a high leak-expression rate and thus a high permanent cost for the cell, limiting its growth prospect under all conditions.

1.1. Summary of the inducer exclusion mechanism

Both in *Saccharomyces cerevisiae* and in *E.coli* diauxie is the result of an inhibition of the secondary metabolism when the primary nutrient is taken up. The basic mechanism is that uptake of the primary nutrient coincides with the production of repressors that prevent directly or indirectly that the genes necessary to import other sugars are expressed. Formally, the mechanisms for *Saccharomyces cerevisiae* and *E.coli* are very similar. In yeast the repressor acts directly on the secondary metabolic genes (Venturelli et al., 2015). In *E.coli*, which is the focus of this contribution, uptake of glucose coincides with the de-phosphorylation of the enzyme $\mathrm{EIIA^{glc}}$. Since dephosphorylation is directly coupled to glucose uptake, the concentration of dephospho-$\mathrm{EIIA^{glc}}$ is a proxy for the uptake rate of glucose. Within the cell dephospho-$\mathrm{EIIA^{glc}}$ is thought to repress uptake of the secondary nutrient in two principal ways: (*i* It mediates the repression of secondary carbon sources via (*i* direct interaction with permeases for secondary sugars (inducer exclusion); (*ii*) it represses the metabolic genes of the secondary metabolism (carbon catabolite repression). In order to maintain the ability of the cell to take up glucose, dephospho-$\mathrm{EIIA^{glc}}$ is continuously re-phsophorylated via the PTS phospho-relay. Therefore, the repression of the secondary metabolisms is quickly eased when the rate of glucose uptake is reduced.

In bacteria, metabolic genes are often regulated via a de-repression motif, as in the case of the *lac* operon: the expression of *lac* is repressed by the *lac* repressor that binds upstream of the *lac* operon and thus prevents its expression. This *lac* repressor is displaced by allolactose which therefore effectively acts as an activator for the synthesis of the genes necessary for lactose utilisation. This de-repression would lead to a "deadlock" state where the cell cannot react to, i.e. "sense", external lactose if it does not have lactose permease already. That these de-repression motifs can work anyway is because *lac* is expressed at a constitutive, low, leak rate. Low level leak import of lactose can then induce the lactose metabolism.

If glucose and lactose is in the system, then $\mathrm{EIIA^{glc}}$ prevents this positive feedback loop of *lac* activation via inducer exclusion and carbon catabolite repression. As levels of $\mathrm{EIIA^{glc}}$ decline, the repression mechanism becomes less efficient and the secondary permease can be induced.

The induction of such systems can be shown to be bistable (Chu, 2015) switching rapidly from fully on to fully off, in the sense that there is a threshold number of permeases above which lactose is taken up. Below this threshold value the metabolic system will not be induced. In the case of *E.coli lac* this threshold number is about 300 permeases (Choi et al., 2008).

2. Results

2.1. Mathematical model

To model the switch we start with a master-equation approach. We view the number of permeases of the secondary nutrient as a read-out for a sensor detecting the concentration of the primary nutrient by "measuring" the abundance of $\mathrm{EIIA^{glc}}$ in the cell. If there are more than a certain threshold number of permeases, then we consider the secondary metabolism to be switched on, otherwise it is off.

Momentarily ignoring switching between the activated and de-activated state, we denote the number of permeases of the secondary metabolism by n, the number of secondary nutrient molecules by l, and the number of $\mathrm{EII^{glc}}$ by R; see Table 1 for a summary of all symbols used. Secondary nutrient is taken up by individual permeases; the uptake of primary nutrient is not explicitly represented in the model. However, in the PTS system uptake of the primary nutrient coincides with the de-phosphorylation of $\mathrm{EIIA^{glc}}$. In the model this is represented by the production (de-phosphorylation) of R at a rate α. R is also removed (by phosphorylation) with a rate δ. Additionally, R binds with n (rate constant k_1^0), which de-activates the permease. We assume here that the R-n compound is very stable and does not decay within relevant time-scales. Fig. 1 represents the model graphically.

If we denote by $P_{R,n,l}(t)$ the probability to observe the system with R molecules of $\mathrm{EII^{glc}}$, n permeases, and l molecules of imported lactose at time t then these interaction can be formalised by the following master equation:

Table 1
Explanation of the symbols used.

Symbol	Biological meaning
R	Dephospho-EIIA^{glc}
n	Number of permeases of secondary nutrient (e.g. LacY)
l	Number of secondary nutrient molecules in cytoplasm
ϵ	Fold-change of expression rate when secondary metabolism is activated.
N	Threshold number of permeases needed to switch on secondary metabolism
k_2	Expression rate of secondary permeases
k_1^0	Rate of R binding with n and thus de-activating n
k_1	Shorthand for $R{\cdot}k_1^0$
δ	Rate of re-phosphorylation of dephospho-*EIIA*^{glc} to EIIA^{glc}
α	Rate of de-phosphorylation of EIIA^{glc}
ζ	Rate of secondary nutrient in cell
γ	Uptake rate of secondary nutrient into in cell

$$\dot{P}_{R,n,l} = k_1^0(R+1)(n+1)P_{R,n,l} + k_2 P_{R,n-1,l} - (k_1^0 Rn + k_2)P_{R,n,l} + \alpha(P_{R-1,n,l} - P_{R,n,l}) + \delta((R+1)P_{R+1,n,l} - RP_{R,n,l}) + \gamma n P_{R,n,l-1} + \zeta(l+1)P_{R,n,l+1} - (\gamma n + \zeta l)P_{R,n,l}$$

Here, we have suppressed the time dependence of the probability to simplify notation. The first line of the above equation models the removal of a permease by binding with the repressor R; this happens with a rate constant of k_1^0. We assume here that R binds to the permeases permanently. The two terms containing the expression rate k_2 represent the production of the permease in the cell. The terms in the second line represent production of R with a rate of α and removal with a rate of δ. The repressor R represents EIIA^{glc} and its production is the rate of de-phosphorylation due to glucose uptake. The rate α is therefore strictly a function of the external glucose concentration. The parameter δ is then the spontaneous re-phosphorylation rate. Finally, the terms in the third line represent uptake and removal of lactose with rates γ and ζ respectively.

A notable omission from the model is the direct genetic regulation of secondary metabolism via cAMP. This control mechanism is redundant and does not seem to add any significant effect with regards to the question asked here (Chu and Barnes, 2016). Moreover, there is experimental evidence (Inada et al., 1996; Bettenbrock et al., 2006; Görke and Stülke, 2008) suggesting that the repression of the metabolic genes in *E.coli* is of secondary importance for diauxic growth. Therefore and for reasons of model parsimony we will concentrate exclusively on direct inducer exclusion here.

In order to be able to obtain analytical results from the model, we will now simplify the master-equation. By applying two key simplification steps we will obtain a standard birth-death process. **Step 1:** The dynamics of l does not feed back on either the number of permeases n or the number of EIIA^{glc}. Hence, we can remove the relevant terms from the equation by summing over all l.

Step 2: The de-phosphorylation of EIIA^{glc}, i.e. production of repressor R is tied to the uptake of glucose which is fast compared to gene expression. Re-phosphorylation rates must be of the same order as the de-phosphorylation rates in order to guarantee sufficient concentrations of phospho-EIIA^{glc} in the cell. This adds high frequency noise to R. The abundance of R also co-varies with fluctuations in the number of glucose specific permeases in a cell. In cells growing exponentially on glucose these fluctuations will be related to the growth rate and the peak expression rate of the glucose permease. While slow compared to the high frequency component, this second source of noise is fast compared to the time between typical leak-expression events of the repressed metabolic genes of the secondary metabolism.

We therefore assume that EIIA^{glc} is in a quasi steady state (QSS) and we replace the number of R by their mean $\overline{R}$ in the master equation. As a further simplification, we note that the mean abundance of R is high with $\overline{R} \gg 1$, hence $\overline{R} + 1 \approx \overline{R}$. Finally, we assume that re-phosphorylation of the repressor EIIA^{glc} is high compared to the leak expression of permease, i.e. $\delta \gg k_1^0 n$. This latter assumption means that binding to permeases is a negligible sink for EIIA^{glc}. It is justified by the high turnover rate of metabolites compared to gene products.

For simplicity we will henceforth omit the over-bar in $\overline{R}$ when denoting the average number of EIIA^{glc}. The above approximations then lead to a birth-death process for our system:

$$\dot{P}(n,t) = k_1^0 R(n+1)P(n+1,t) + k_2 P(n-1,t) - (Rnk_1^0 + k_2)P(n,t) \quad (1)$$

This master equation can be solved leading to a Poisson distribution for n.

$$P(n,t) = \frac{\lambda(t)^n \exp(-\lambda(t))}{n!}, \quad \text{where} \quad \lambda(t) = \frac{k_2}{Rk_1}(1 - \exp(-Rk_1^0 t))$$

This solution is of limited use for the present purpose. We are interested in the amount of time the system spends being activated or not, i.e. above or below the threshold concentration of permeases.

The activation/deactivation time is formally a mean first passage time (MFPT). For the birth-death process in Eq. (1) this time can be calculated exactly and provides formulas for the expected time for the system to be switched on and off. Specifically, we will consider the secondary metabolism to be activated if there are more than N permeases; otherwise if $n \leq N$ it is deactivated or "off" (see Fig. 3 for a schematic explanation). Whenever the system crosses this threshold, we assume that the expression rate for the secondary permeases switches abruptly from low to high (or vice versa). This means that there are two parameters for the expression rate corresponding to the leak rate and the expression rate of the induced gene.

For convenience, but in slight abuse of notation, we will denote the expression rate of the gene coding for permeases by k_2. In those cases

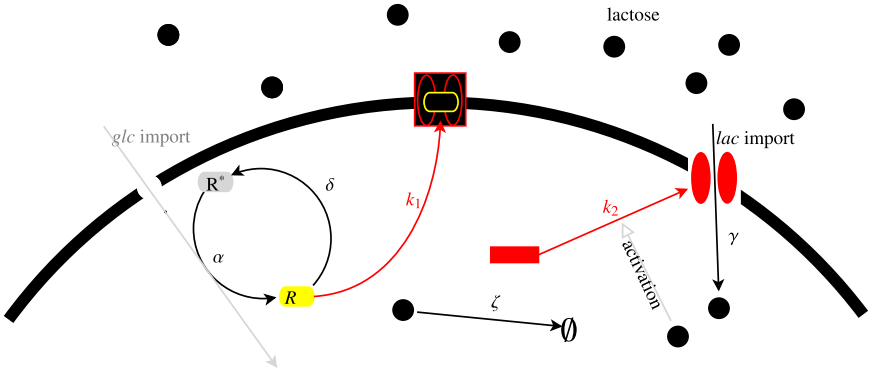

Fig. 1. Schematic drawing of the model. The grey elements are implicit to the model only. The black elements are in the full model only and the coloured elements are contained in the reduced model in Eq. (1). (For interpretation of the references to color in this figure legend, the reader is referred to the web version of this article.)

below, where the induced rate and the leak expression rate appear in the same formula, we will denote the activated value by k_0. In many cases below, we will write k_0 as an ϵ-fold multiple of the leak expression rate. We will then write $k_0 = \epsilon k_2$. The parameter ϵ specifies the factor by which the leak expression rate is increased when the gene is fully induced.

2.2. Mean time to switch

In this section we will calculate the MFPT. This will then provide us with the rates of switching between the activated and the de-activated state and will allow us to calculate the long-term probability of finding the secondary metabolism switched on or off depending on R.

We first compute the MFPT to reach the threshold number of N permeases when starting from a state n=x. To do this we use an approach described by Bressloff, sec. 6.6 and start from the backwards version of the master Eq. (1). The general form of this backward equation for a birth death process is (Bressloff):

$$\dot{P}(n, t|n_0, 0) = \omega_+(n_0)[P(m, t|n_0 + 1, 0) - P(n, t|n_0, 0)] + \omega_-(n_0)[P(n, t|n_0 - 1, 0) - P(n, t|n_0, 0)] \quad (2)$$

The backward equation is equivalent to the standard master equation, but is formulated with respect to the position at time t=0. In our particular problem, the generalised rates $\omega_\pm$ are $\omega_+ = k_2$ and $\omega_-(n) = nk_1 = nRk_1^0$.

The basic idea of calculating the MFPT is to erect an absorbing boundary condition at the point b=N. Absorbing here means that the system, once it has reached this point, cannot go back to previous states any more. Biologically, we will then identify this boundary with the threshold number of permeases needed to switch on the secondary metabolism.

Given this absorbing boundary condition, we can now formulate the probability $S(t, n_0)$ of finding the system in any of the sites $1 \ldots N-1$ at time t given that we started at n_0 at time t=0.

$$S(n_0, t) := \sum_{n=a}^{b} P(n, t|n_0, 0)$$

Here a is the reflecting boundary of the interval. It can then be seen (Bressloff,) that

$$T(n_0) = \langle T \rangle = \int_0^\infty S(n_0, t)\, dt$$

Summing over all n in the master Eq. (2), we obtain an equation for S.

$$\frac{dS(n_0, t)}{dt} = \omega_+(n_0)[S(n_0 + 1, t) - S(n_0, t)] + \omega_-(n_0)[S(n_0 - 1, t) - S(n_0, t)]$$

We can now integrate over all t, to obtain a formula for the mean time to absorption:

$$-1 = \omega_+(n_0)[T(n_0 + 1) - T(n_0)] - \omega_-(n_0)[T(n_0) - T(n_0 - 1)] \quad (3)$$

If we now introduce the helper function $U(n)$ defined by

$$U(n) := T(n) - T(n - 1) \quad (4)$$

, then we obtain a recursive relationship for $U(n_0)$:

$$\omega_+(n_0)U(n_0 + 1) - \omega_-(n_0)U(n_0) = -1$$

The MFPT problem can be solved in general using those equations by imposing the relevant boundary conditions to the problem. Here we are interested in two different solutions. The MFPT $T_+(x)$ from the de-activated state to the activated state and the MFPT $T_-(x)$ from the activated state to the de-activated state. These correspond to the mean waiting times for the system to switch itself on and off respectively. The de-activation time requires the left boundary a to be reflecting, and the right boundary (b) corresponding to the activation threshold to be absorbing. *Vice versa* the waiting time to transition from the activated state to the de-activated state is the MFPT to reach the absorbing point $a < b$, where b is a reflecting point. Here, we will choose the reflecting boundary of the activated state to be located at infinity and the reflecting boundary of the de-activated state corresponds to 0 permeases, i.e. for the activated state we will choose, a=N and $b \to \infty$ and for the de-activated state, a=0 and $b = N - 1$ where N is the threshold.

2.3. MFPT with $a < b$ and a absorbing and b reflecting

We will first compute the deactivation time. The point a is absorbing; b is reflecting and $a < b$. The reflecting boundary condition implies that $T(b + 1) = T(b)$. We can now use this to calculate $U(b)$ from Eq. (3), which implies a recursive solution for $U(n)$ for any n:

$$U(n) = \frac{1}{\omega_-(n)} + \frac{\omega_+(n)}{\omega_-(n)} U(n + 1)$$

The recursive sequence is truncated at the reflecting boundary given by n=b

$$U(b) = \frac{1}{\omega_-(b)} \quad \text{(Boundary condition)}\, U(b - 1) = \frac{1}{\omega_-(b - 1)} + \left[\frac{\omega_+(b - 1)}{\omega_-(b - 1)} U(b)\right] = \frac{1}{\omega_-(b - 1)} + \left[\frac{\omega_+(b - 1)}{\omega_-(b - 1)} \frac{1}{\omega_-(b)}\right] U(b - 2)$$
$$= \frac{1}{\omega_-(b - 2)} + \left[\frac{\omega_+(b - 2)}{\omega_-(b - 2)} \frac{1}{\omega_-(b - 1)} + \frac{\omega_+(b - 2)}{\omega_-(b - 2)} \frac{\omega_+(b - 1)}{\omega_-(b - 1)} \frac{1}{\omega_-(b)}\right]$$

This leads to a general formula for any $U(n)$:

$$U(n) = \sum_{i=n}^{b} \psi(n, i), \quad \text{where} \quad \psi(n, i) := \frac{1}{\omega_-(i)} \left(\prod_{j=n}^{i-1} \frac{\omega_+(j)}{\omega_-(j)}\right)$$

The left absorbing boundary condition means that the waiting time beyond the transition point is zero, i.e. $T(a - 1) = 0$. This can be used to truncate the recursive formula for $T(n)$ in Eq. (4).

$$T(n) = U(n) + T(n - 1) = U(n) + U(n - 1) + \cdots + U(a) = \sum_{k=a}^{x} U(k)$$

Altogether, we then obtain the final formula for the mean first passage time at a:

$$T(n) = \sum_{y=a}^{n} \sum_{j=y}^{b} \left(\frac{1}{\omega_+(j)} \prod_{i=y}^{j} \frac{\omega_+(i)}{\omega_-(i)}\right)$$

This formula is general, but not very useful by itself. For the particular question we are interested in calculating the rate of switching between the two states. For this, we need to evaluate the expected time for the system to remain switched on after having transitioned into this state. This time is the mean first exit time from the activated state when starting from just above the threshold. For this case the formula reduces considerably in complexity. Setting $\omega_-(n) = k_1 n$ and $\omega_+ = k_2$ we obtain for ψ.

$$\psi(y, j) = \frac{k_2^{j-y} k_1^{y-j} (y - 1)!}{(j - 1)! k_1 j}$$

It is possible to evaluate the first sum for $b \to \infty$:

$$T_-(a) = \sum_{j=a}^{\infty} \psi(a, j) = \frac{1}{k_1} e^{\frac{k_2}{k_1}} \left(-\Gamma\left(a, \frac{k_2}{k_1}\right) + (a - 1)!\right) \left(\frac{k_1}{k_2}\right)^a$$

This is the mean waiting time to deactivate when starting from just beyond the threshold.

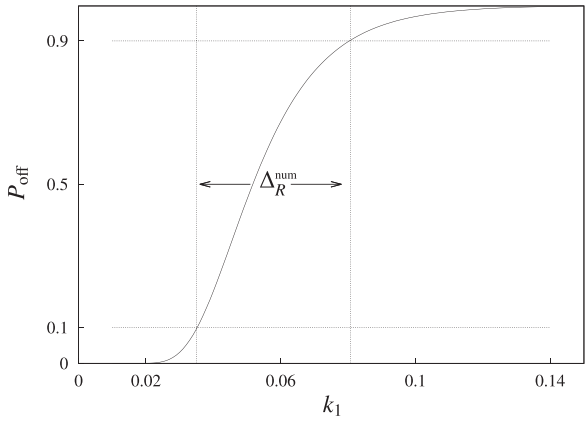

Fig. 2. P_{off} as in Eq. (7) as a function of k_1 for k_2=0.5, $\epsilon = 1$ and b=10. The uncertainty Δ_R^{num} is the distance between the points where P_{off} reaches 0.1 and 0.9 respectively.

2.4. Calculating the case for a reflecting, b absorbing, $a < b$

In a similar way, we now compute the probability of reaching $b + 1$ starting from x when a is a reflecting boundary. In this case, the boundary conditions are:

$$T(b+1) = 0 \quad T(a-1) = T(a)U(b+1) = -T(b) \quad U(a) = 0$$

In close analogy to above we calculate the mean first passage time by first developing a recursive solution for $U(n)$ taking into account the boundary conditions. We obtain:

$$U(n+1) = -\frac{1}{\omega_+(n)} + \frac{\omega_-(n)}{\omega_+(n)}U(n) = \cdots = -\sum_{z=a}^{n-1}\phi(z, n-1)$$

Here we define

$$\phi(i,j) := \frac{1}{\omega_+(j)}\prod_{l=i+1}^{j}\frac{\omega_+(l)}{\omega_-(l)}$$

Using this we can then further establish a general formula for the MFPT

$$U(n) = T(n) - T(n-1)\,T(n-1) = T(n) - U(n) = T(n+1) - U(n+1) - U(n)$$
$$= \cdots T(n) = \sum_{i=n+1}^{b} U(i)$$

Substituting in the formal solution of $U(n)$ we get.

$$T(n) = \sum_{i=n+1}^{b}\sum_{z=a}^{i-1}\phi(z, i-1)$$

Similar to above, we are interested in the mean first exit time from the de-activated state when starting from just below the threshold. Setting $n = b - 1$ and substituting our rates for $\omega_\pm$ we obtain an expression for the relevant time.

$$T_+(b-1) := k_1^{b-1}k_2^{-b}e^{\frac{k_2}{k_1}}\Gamma\left(b, \frac{k_2}{k_1}\right) = k_1^{b-1}k_2^{-b}e^{\frac{k_2}{k_1}}\int_{\frac{k_2}{k_1}}^{\infty} s^{b-1}e^{-s}ds \tag{5}$$

2.5. Probability to be de-activated

We can now calculate the probability of the system being in the "off" state. If `down`is the rate of the system to transition from the activated state to the off state and `up`the rate from the off state to the activated state, then the probability to be in the off state is given by:

$$P_{\text{off}} = \frac{\frac{1}{\text{up}}}{\frac{1}{\text{up}} + \frac{1}{\text{down}}} = \frac{\text{down}}{\text{up} + \text{down}}$$

Assuming now that the threshold is at n=N, then the rate `up` equals $T_+^{-1}(N-1)$, the inverse of the MFPT to reach the threshold when starting from just one molecule less than the threshold. Similarly, the rate `down` is $T_-(N)^{-1}$ the inverse of the MFPT to drop below the threshold when starting from just one molecule above the threshold. The expressions for $T_\pm$ have been calculated above. Writing k_0, the activated expression rate of the permeases, as a fixed multiple of the leak rate, $k_0 = \epsilon k_2$ ($\epsilon \geq 1$) we obtain an expression for the probability to be switched off:

$$P_{\text{off}} = \left(\frac{\Gamma(N) - \Gamma\left(N, \frac{\epsilon k_2}{k_1}\right)}{\Gamma\left(N, \frac{k_2}{k_1}\right)}\epsilon^{-b}e^{\frac{(\epsilon-1)k_2}{k_1}} + 1\right)^{-1} \tag{6}$$

$\Gamma(x)$ and $\Gamma(x, y)$ are the Γ function and the upper incomplete Γ function respectively.

The expression in Eq. (6) is the probability that given a certain number of R the system is in its de-activated state. The number R, which represents the number of EIIA^{glc}, is not explicitly stated in this expression, but is contained in the parameter k_1, which has previously been defined as a shorthand for Rk_1^0. As written Eq. (6) is not very illuminating, but for some special cases the expression can be simplified significantly.

2.6. Accuracy of switch in the limiting case of $\epsilon = 1$

We will first consider the limiting case of $\epsilon = 1$. Then the expression for the probability in Eq. (6) reduces to a ratio between two Γ functions.

$$P_{\text{off}} = \frac{\Gamma\left(b, \frac{k_2}{k_1}\right)}{\Gamma(b)} = \frac{\int_{\frac{k_2}{k_1}}^{\infty} s^{b-1}e^{-s}ds}{\int_0^{\infty} s^{b-1}e^{-s}ds} \tag{7}$$

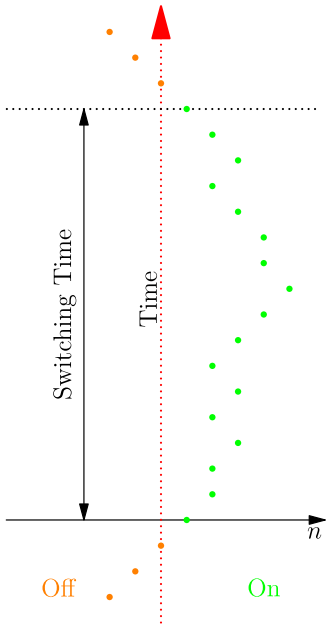

Fig. 3. A schematic illustration of the switching time. The time to deactivate the system is the period between the system reaching n=N from below until it reaches the threshold again.

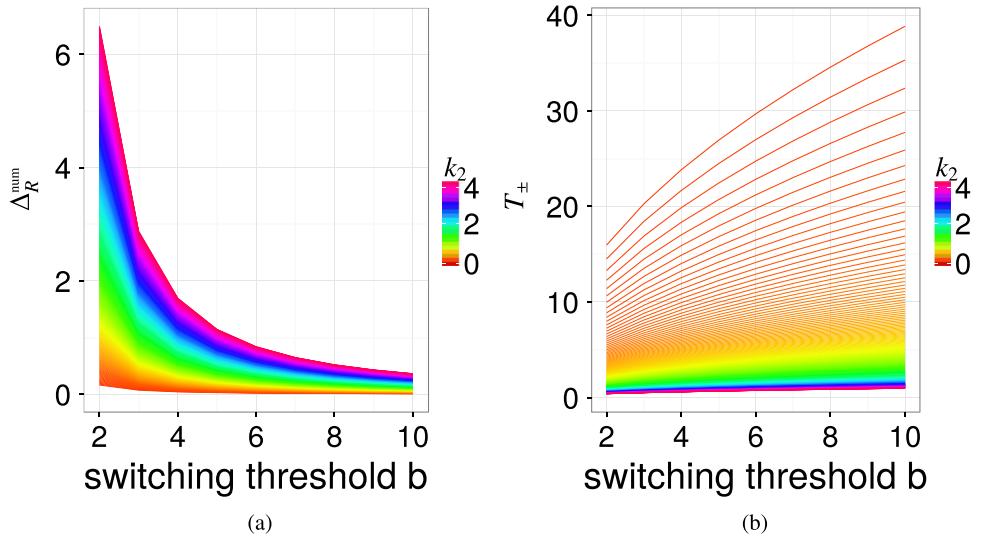

Fig. 4. (a) The uncertainty Δ_R calculated numerically as the distance between $P_{off} = 0.1$ and $P_{off} = 0.9$. (b) The switching time at $P_{off} = 1/2$ for a a number of different k_2 and $\epsilon = 1$. Note that by choice of the parameter k_1 we have $T_- = T_+$.

This function shows a sigmoidal transition from 0 to 1 as k_1 crosses the threshold (Fig. 2). Recall that $k_1 := Rk_1^0$ with k_1^0 constant. Hence, the control parameter here is the abundance of R. For low R, corresponding to low glucose uptake rates, the probability for the secondary metabolism to be on is almost 1, as expected. Equally, for high R the system is almost certainly switched off. There is a transition area Δ_R in-between, where the system could be either switched on or switched off (Fig. 3).

For the cell, Δ_R corresponds to a region where its internal state cannot be accurately controlled in response to a change of environmental conditions. At the level of the population, this would result in a bimodal distribution, whereby some cells have the secondary metabolism activated, while others not. The existence of this area can be interpreted as a consequence of the fundamental limitation of the sensing apparatus that is implicit in the regulatory network modelled here. It is well known that biological systems are limited in their ability to determine molecular concentrations accurately. The present case represents a binary sensing problem, i.e. the cell needs to establish whether or not R is above or below a certain threshold. Consequently, sensing inaccuracies only manifest themselves close to a threshold. Inaccuracies are irrelevant far away from the threshold, i.e. for very low or very high R.

In the limiting case of $\epsilon = 1$ it is possible to find an analytic expression, Δ_R^{sym} for the width of Δ_R. We now define the *switching point* as the value of k_1 where the sigmoid function has maximal slope for a given k_2 and N. Since the denominator in Eq. (7) does not depend on k_1, the switching point is the maximum of the first derivative of the enumerator and is located at $k_1 = k_2/(N+1)$. Here we define Δ_R^{sym} as the distance between the inflection points of the sigmoid function. We find those by solving the equation $d^3P_{off}/dk_1^3 = 0$ for k_1. This yields two positive solutions. The difference between those is:

$$\Delta_R^{sym} = \frac{2k_2}{(N+2)^{\frac{3}{2}} - (N+2)^{\frac{1}{2}}}$$

The uncertainty is proportional to k_2. Consequently, a higher leak rate means that there is a larger range of parameters where the secondary metabolism can be either switched on or off. On the other hand, the uncertainty is also inversely correlated to N. Biologically this has a concrete interpretation: Switching at lower abundances of R, i.e. at lower concentration of glucose, necessarily increases the uncertainty Δ_R.

For $\epsilon > 1$ there is no useful analytical expression for the width of Δ_R. We define the numerical value of the width, Δ_R^{num}, as the distance between some threshold values for P_{off}. Throughout this contribution we keep these values fixed at 0.1 and 0.9 (see Fig. 4). The two measures Δ_R^{num} and Δ_R^{sym} are not numerically identical, but it will become clear below that they both show the same scaling behaviour with respect to key-parameters; see Fig. 5.

2.7. Time required to switch

The long-term probability to find the system switched on or off (Eq. (6)) does not provide any information about the time required to switch, i.e. how often the system switches between activated and de-activation. This information is contained in the expressions for the MFPT above. We now consider the time to switch at the above defined switching point where $k_1 = k2/(N+1)$. Substituting this value into the full formulas for the MFPT one can see that $T_\pm \sim k_2^{-1}$.

Hence, while the accuracy of the switch, $\Delta_R \sim k_2$, the speed of switching is proportional to the inverse of k_2 at the switching point.

2.8. The case $k_0 > k_2$: activated expression is higher than leak

Once we relax the condition $\epsilon = 1$ then the system is no longer amenable to analytical treatment and numerical analysis is necessary. We found that the qualitative dependence of Δ_R on the threshold N can be recovered for $\epsilon > 1$. To confirm this we performed numerical simulations (see Fig. 5a). We kept the transition threshold fixed (at $N = 5, 10, 15, 20$). Then we set $\epsilon = 3$, chose a value of k_2 and calculated numerically the values of k_1 where the probability of being switched off are 0.1 and 0.9 respectively. We called the difference between these two values Δ_R^{num} and plotted it for different values of the threshold N in Fig. 5a; analogously we plotted Δ_R^{num} as a function of k_2 for different values of the threshold in Fig. 5b. These graphs show the same qualitative dependence as in the case of $\epsilon = 1$

In a similar way we determined the switching time as a function of k_2. To this end we determined the value of k_1 such that $P_{off} = 1/2$; from this we then calculated the transition-time using Eq. (5). Fig. 5c shows the inverse of the switching time for a number of threshold values. As expected it is a straight line, confirming that the switching time is inversely proportional to k_2. By construction, the values of T_- are exactly the same as T_+ hence only one is shown here.

Note that the linear relationship between k_2 and the switching time and uncertainty respectively will only be retained if the activated expression rate $k_0 = \epsilon k_2$, i.e. is a fixed multiple of the leak expression rate. If k_0 is kept fixed, while k_2 is varied then there is no longer a

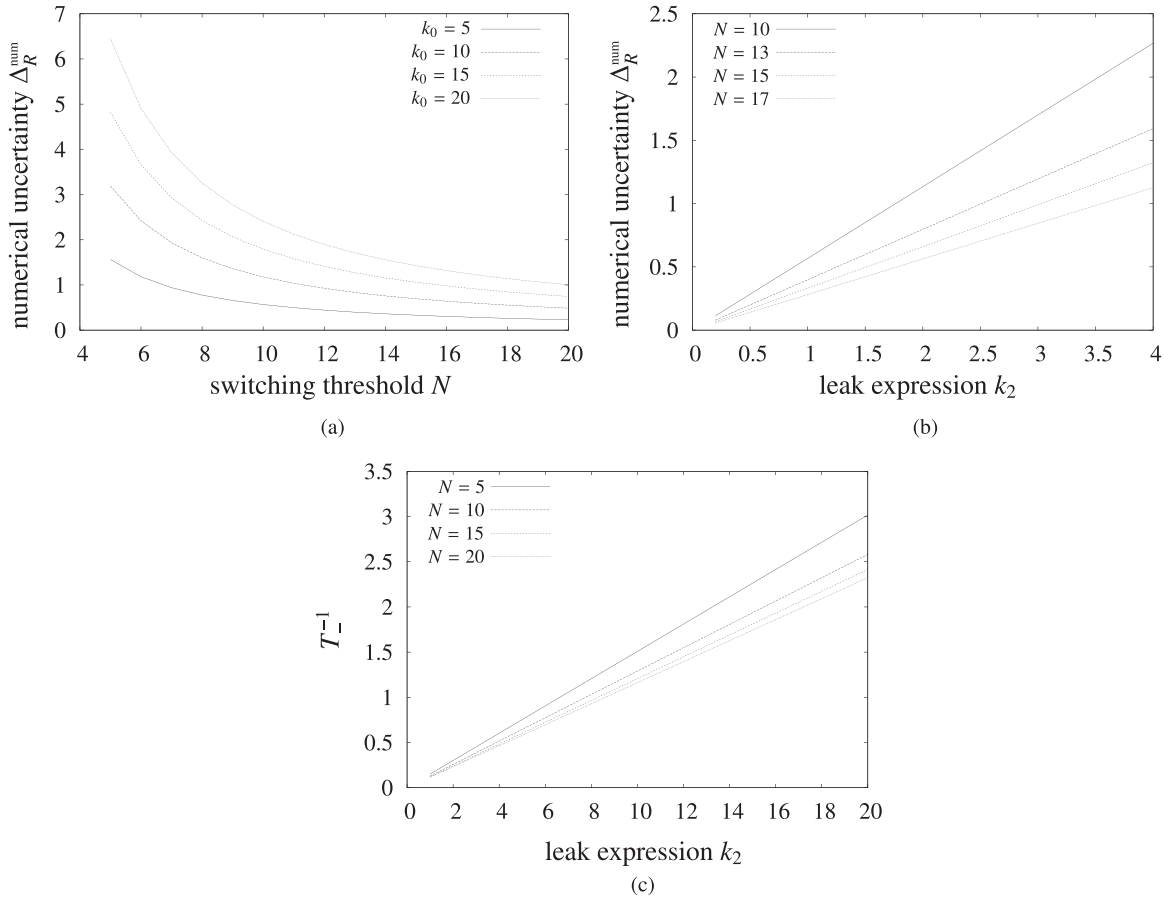

Fig. 5. (a) The uncertainty as a function of the switching threshold. (b) Same, but the leak expression rate k_2 is varied while keeping the peak expression rate constant k_0 at a fixed multiple of the leak. See main text for details. The graphs (c) show the inverse of the expected time to switch on at the point where the probability of being on and off is equal. The parameter $k_0 = 3k_2$.

simple relationship between k_2 and the uncertainty. For some parameters Δ_R^{num} can even decrease with increasing k_2. That the proportionality cannot be retained in the case of a fixed k_0 is apparent from the expression defining P_{off} in Eq. (7).

3. Discussion

Here we modelled a PTS-like system for the control of inducer exclusion as a biological binary sensor. Due to inherent noise of the system, specifically the fluctuations in the number of permeases, the system is fundamentally limited in its accuracy. Since the PTS system is a binary detector, the limitations become only relevant in the vicinity of the transition threshold.

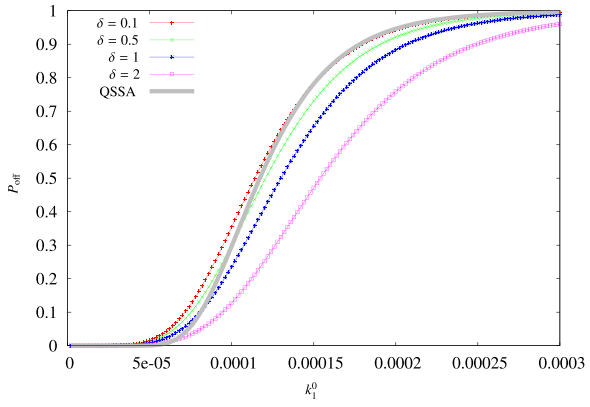

Fig. 6. Testing the limits of the QSSA. The grey curve shows a numerical solution for the master equation using $k_2 = 0.5$, $\epsilon = 1$ and R=400. The along the horizontal axis $k_1{}^0$ is varied. The coloured lines show the probability for the system to be switched on after 70 time units assuming for different values of the decay rate δ. (For interpretation of the references to color in this figure legend, the reader is referred to the web version of this article.)

3.1. Time-accuracy trade-off

The inaccuracy Δ_R is the manifestation of a general limitation of the ability of cells to establish the concentration of molecules internally or in their environments. Theoretically, it is to be expected as a consequence of a more general limitation of biological systems to sense their environment, as first proposed by Berg and Purcell (1977). Experimentally it would manifest itself as a population heterogeneity with respect to the induction state of the secondary metabolism during the lag-phase. At certain low concentrations of the primary nutrient the population would consist of cells that have an activated secondary metabolism and some that do not. Such heterogeneity has been observed experimentally (Boulineau et al., 2013) and has even been suggested as the fundamental reason for the lag-phase (Kotte et al., 2014). From our minimal model it is not possible to make quantitative predictions about the amount of heterogeneity to be expected based on the sensing limitations inherent in the PTS system. It is of course conceivable that effects other than sensor limitations can also explain these effects. The possibility that there is a connection between the well known Berg-Purcell limit (Berg and Purcell, 1977) of biological sensors and the equally well known effect of diauxic growth remains intriguing.

According to our model a certain degree of inaccuracy is unavoidable, but Δ_R can be reduced by an appropriate choice of parameters. Our model predicts that there is a trade-off between the width of Δ_R

and the parameter k_2, i.e. the time required to switch. The width of Δ_R is proportional to k_2, but the time to switch between the activated and the de-activated state is inversely proportional to k_2. A moderate inaccuracy Δ_R is unlikely to be detrimental to the cells. It prevents the population from switching collectively at a particular time in unison, but is also a source of heterogeneity, which may even be beneficial evolutionarily especially with respect to bet-hedging strategies (King and Masel, 2007; Müller et al., 2013).

3.2. Trade-off between the efficiency and the speed

The second trade-off emerging from our model is between the efficiency of switching and the length of the lag-phase. A maximally efficient sensor would be able to detect the precise point when the primary nutrient runs out and then switch to the secondary nutrient immediately. Within our model this is not possible. Informally, this can be seen as follows: Precise switching would imply that the secondary metabolism remains repressed by a single molecule of R and that upon the removal of the last R the secondary metabolism is immediately active. This is only possible if there is at most a single permease for the secondary carbon source in the cell which implies that $k_2 \to 0$. In this limit the waiting time for the next leak expression event—and also the time to reach the threshold—diverges.

This informal argument already suggests that there is a trade-off between the speed with which the system is able to switch and the efficiency of control. This intuition can be confirmed formally. Using the simplified model from above with $\epsilon = 1$ we can define the switching point as the point of maximum slope of the function $P_{\text{off}}(k_1)$ located at $k_1 = k_2(N+1)^{-1}$. Writing now $k_1 = Rk_1^0$, we obtain the number of R required to switch:

$$R_{\text{sw}} = \frac{k_2}{k_1^0}\cdot\frac{1}{N+1}$$

Noting that the abundance of R will be typically very large we find that $k_1^0 \ll 1$. A small value of R_{sw}, i.e. switching at low external concentrations of the primary nutrient, therefore relies on k_2 small or N large. A trade-off arises here because both of these possibilities entail that $T_{\pm}$ are high (c.f. Eq. (5)). Hence, efficient switching entails slow switching. Note that efficient switching also entails high accuracy switching, i.e. Δ_R small.

A certain degree of premature switching to the secondary nutrient is therefore unavoidable and a direct consequence of the limitations of stochastic systems. Interestingly, our minimal model reproduces the empirical relationship found by Wang et al. (2015) between early switching and short lag-phase. Note that the Wang study focussed not on bacteria but on yeast which are regulated differently. One possibility is of course that the relationship measured by Wang et al. is due to some other constraints in the cell and unrelated to the trade-off established by our model. On the other hand, since the trade-offs we found are a consequence of the fundamental limitations of stochastic sensors we expect that they are not dependent on the details of the system, but appear in many biological sensors.

3.3. Cost

Computation in stochastic systems can only happen when the system is kept out of equilibrium by dissipating energy (Bennett, 1982). Sensing is a form of computation and as such requires energy dissipation as well. In the particular case of our model, one important contributor to cost in energy is the leak expression of permeases, which is a constitutive basal expression rate. Permeases are synthesised at this rate independently of the presence or absence of the relevant carbon source. This comes at a resource cost for the cell in the form of a direct metabolic cost of amino acid synthesis, sequestration of ribosome during translation but also spatial costs due to permeases occupying space on the cell surface. A high leak expression rate therefore draws permanently resources from the cell, thus reducing long-term growth potential on any carbon source. From the model one would therefore predict a trade-off between short lag-phases and long-term growth potential. Such a trade-off between the ability to switch and the growth speed is well established experimentally (Schuetz et al., 2012). Recent simulation models using more detailed models confirm this.

3.4. Limitations to the model

Crucial for the derivation of the birth-death process was the assumption that the repressor R is in a QSS with respect to the expression dynamics of the secondary nutrients. This can be justified by the fact that levels of R are coupled to the uptake of glucose which fluctuates over a time-scale much faster than the typical time-scale of leak-expression. In those cases, any fluctuations of R are averaged out. The QSSA also rests on the assumption that the mean abundances of R, and thus the mean uptake rate of glucose, changes slowly over time. Experimentally, this can be realised in chemostats where glucose concentrations can be kept fixed. Sufficiently low concentrations of glucose then allow co-utilisation of glucose and lactose (Lendenmann et al., 1996; Lendenmann and Egli, 1995), consistent with the prediction of our model.

The opposite extreme of the QSS model is an instantaneous change of the glucose uptake rate from some very high value to nothing; see Chu and Barnes (2016) for a detailed stochastic simulation model of this scenario. An instantaneous model is trivially not compatible with bistability (in the sense of co-utilisation of primary and secondary nutrients). In this scenario, immediately after the switch lactose expression is completely repressed and no growth is possible. Cells need to wait for the lactose metabolism to be expressed, while they continue to express glucose permeases in the meantime. Those cells that eventually activate lactose through leak expression will then resume growth fuelled by lactose. Yet, there will be cells that do not express a secondary metabolism and perhaps enter into a dormant state.

In batch-growth experiments, the QSSA will be an approximation. Depending on the specifics of the set-up towards the end of the first growth-phase changes of the concentrations of the primary nutrient may be non-negligible. The principle conclusions of our QSS model remain valid even then. To check this, we extended our model and allowed the repressor R to decay. Using the Prism model checker (Kwiatkowska et al., 2001) we calculated the probability of the system to be switched on after 70 time units given various decay rates for R. A vanishing decay rate would correspond to the perfect QSS (grey curve in Fig. 6). As expected, for small decay rates the QSSA is a good approximation, but less so for large decay rates corresponding to fast reduction of R. Note that the qualitative shape of the probability distribution remains unchanged over the time-scale considered. However, once one departs from the QSSA too fast, the time-dependence of the probability will become dominant and the systems dynamics will increasingly resemble that of the instantaneous switch.

Further quantitative errors are introduced by other approximating assumptions of the birth-death process, including: (*i* The R-n compounds is vanishingly small whereas in real systems $R - n$ compounds may decay in finite time. (*ii*) The activation threshold b is sharp. In reality, activation of sugar metabolisms is a stochastic function of the number of permeases. (*iii*) The translation step during the synthesis of permeases does not add to the noise in the protein signal. LacY is produced in burst of about 35 (Mettetal et al., 2006), thus creating additional fluctuations.

3.5. Testable predictions

The combined effect of those assumptions is that the model underestimates the noise in the system. It is therefore unlikely to be useful in

making quantitative predictions about real bacteria. However, the main qualitative insights we derived, the trade-offs arising from the model, are effects to be expected in real systems because they depend on the stochastic dynamics only. It is a mathematical given that the networks of the type considered would lead to a lag-phase that is driven by limitations to sensing. Qualitatively, the same effects that our model predicts have also been observed in micro-organisms. While encouraging, this does clearly not mean that limitations of sensors are the sole or even dominant cause of the lag-phase. There could be a number of other effects that give rise to the same behaviours.

Validating the predicted effect for cells can, at least partially, be done using extensive computer simulations. Assuming these models represent microbial metabolism and growth in sufficient detail, including a plausible parametrisation, it would be possible to estimate the contribution of sensing uncertainty to the lag-phase. The problem of such simulation models is that they would be computationally very expensive.

An immediate experimental test of the model would be to confirm that in bacteria there is the same relationship between pre-mature switching and the lag-phase that Wang et al. found for yeast. Furthermore, the model affords an important role to the leak rate expression of the permeases. If the model is relevant, then one would expect to be able to observe that changing the leak rate modulates the length of the lag-phase. A further prediction of the model is that the presence of two concomitant sugars shortens the lag-phase relative to the presence of only one secondary sugar. Although, it is conceivable that second order effects based on hierarchies of secondary nutrients could mask this effect (Aidelberg et al.,, Koirala et al., 2015).

4. Conclusion

We used a minimal model of the regulatory network of diauxic growth. This model predicts that there are limitations to the ability of cells to switch from one nutrient to another that arise as a consequence of the limitations of stochastic biological sensors (Mehta and Schwab, 2012; Bialek and Setayeshgar, 2008; Govern and ten Wolde, 2014, 2014). As a consequence of this a number of trade-offs emerge. (*i* We found that accurate (Δ_R small) and efficient (R_{sw} small) switching is only possible at the expense of a long lag-phase. Inaccurate switching may also be the reason for the observed population heterogeneity during the lag-phase. (*ii*) The cell can (over evolutionary times) decrease the duration of the lag-phase, but this implies a permanent metabolic cost penalty on the cell, which limits growth in the long run. In environments where switching between nutrients is infrequent, it will then be beneficial to accept a higher lag-phase (and episodic fitness penalty) in exchange for a better long-term growth rate. In environments that do not see frequent changes of conditions longer lag-phases will be beneficial, while in variable environments shorter lag-phases paired with smaller long-term growth would evolve.

The existence of speed-accuracy-cost trade-offs in biological systems is not a surprise. Similar relationships have been found in a number of contexts now including gene networks (Zabet and Chu, 2010; Chu et al., 2011) or bacterial adaptation systems (Lan et al., 2012). Ultimately, these trade-offs are a consequence of the limitations of Brownian computers (Bennett, 1982).

The significant insight here, therefore, is not so much that sensing the external concentration of the primary nutrient is subject to limitations and trade-offs, but that these trade-offs can explain the well known phenomenon of the lag-phase, which has so far not been thought of as a sensing problem. This is an exciting prospect. If methods from statistical physics can predict design principles of biological systems, then this opens up for substantial progress in a theory-driven biology.

The limitation of sensing may or may not be the sole driver for the evolution of the lag-phase; it may not even be the dominant one. Further research is required in order to establish this. Yet, importantly, the biological consequences indicated by our model are qualitatively consistent with observed behaviours in real cells.

Acknowledgments

I thank Prof. Christian Ray and two anonymous reviewers for their comments, which helped to improve this manuscript.

Appendix A. Code of the PRISM model

```
ctmc

const int nmax = 50;
const double k2l=0.5;
const double k2=0.5;
const double k1=xxx;
const double nT = 10;
    module mixm
n: [0..nmax] init 1;
r: [1..400] init 400;
[t1] n < = nT- > k2l: (n'=n+1);
[t2] n > 0- > n*r*k1 : (n'=n-1);
[t3] n > nT & n < nmax- > k2: (n'=n+1);
[t4] r > 1 - > delta: (r'=r-1);

endmodule
```

Fig. 6 was produced by querying the model using `P=? [true U[70, 70] n< = nT]` for different values of `k1` and `delta` (corresponding to the parameter k_1^0 and δ respectively in the main model).

References

Aidelberg, G., Towbin, B., Rothschild, D., Dekel, E., Bren, A., Alon, U., Hierarchy of non-glucose sugars in Escherichia coli, BMC Syst. Biol., 8 (1). http://dx.doi.org/10.1186/s12918-014-0133-z

Barato, A., Seifert, U., 2015. Thermodynamic uncertainty relation for biomolecular processes. Phys. Rev. Lett. 114, 158101. http://dx.doi.org/10.1103/PhysRevLett.114.158101.

Bennett, C., 1982. The thermodynamics of computation. a review. Int. J. Theor. Phys. 21 (12), 905–940. http://dx.doi.org/10.1007/bf02084158.

Berg, H.C., Purcell, E.M., 1977. Physics of chemoreception. Biophys. J. 20 (2), 193–219. http://dx.doi.org/10.1016/S0006-3495(77)85544-6.

Bettenbrock, K., Fischer, S., Kremling, A., Jahreis, K., Sauter, T., Gilles, E., 2006. A quantitative approach to catabolite repression in Escherichia coli. J. Biol. Chem. 281 (5), 2578–2584. http://dx.doi.org/10.1074/jbc.M508090200.

Bialek, W., Setayeshgar, S., 2005. Physical limits to biochemical signaling., In: Proceedings of the National Academy of Science USA, 102 (29), pp. 10040–10045. http://dx.doi.org/10.1073/pnas.0504321102

Bialek, W., Setayeshgar, S., 2008. Cooperativity, sensitivity, and noise in biochemical signaling. Phys. Rev. Lett. 100 (25), 258101.

Boianelli, A., Bidossi, A., Gualdi, L., Mulas, L., Mocenni, C., Pozzi, G., Vicino, A., Oggioni, M., 2012. A non-linear deterministic model for regulation of diauxic lag on cellobiose by the pneumococcal multidomain transcriptional regulator celr. PLoS One 7 (10), e47393. http://dx.doi.org/10.1371/journal.pone.0047393.

Boulineau, S., Tostevin, F., Kiviet, D., ten Wolde, P., Nghe, P., Tans, S., 2013. Single-cell dynamics reveals sustained growth during diauxic shifts. PLoS One 8 (4), e61686. http://dx.doi.org/10.1371/journal.pone.0061686.

Brückner, R., Titgemeyer, F., 2002. Carbon catabolite repression in bacteria: choice of the carbon source and autoregulatory limitation of sugar utilization. FEMS Microbiol. Lett. 209 (2), 141–148. http://dx.doi.org/10.1016/S0378-1097(02)00559-1, (URL ⟨http://www.sciencedirect.com/science/article/pii/S0378109702005591⟩).

Bressloff, P.C., Stochastic processes in cell biology, Interdisciplinary Applied Mathematics http://dx.doi.org/10.1007/978-3-319-08488-6

Choi, P.J., Cai, L., Frieda, K., Xie, X.S., 2008. A stochastic single-molecule event triggers phenotype switching of a bacterial cell. Science 322 (5900), 442–446. http://dx.doi.org/10.1126/science.1161427.

Chu, D., Barnes, D.J., 2016. The lag-phase during diauxic growth is a trade-off between fast adaptation and high growth rate. Sci. Rep. 6, 25191. http://dx.doi.org/10.1038/srep25191.

Chu, D., Zabet, N., Hone, A., 2011. Optimal parameter settings for information processing in gene regulatory networks. BioSystems 104, 99–108. http://dx.doi.org/10.1016/j.biosystems.2011.01.006, (URL ⟨http://www.cs.kent.ac.uk/pubs/2011/3081⟩).

Chu, D., 2015. In silico evolution of diauxic growth. BMC Evolut. Biol. 15, 211. http://dx.doi.org/10.1186/s12862-015-0492-0.
Deutscher, J., 2008. The mechanisms of carbon catabolite repression in bacteria. Curr. Opin. Microbiol. 11 (2), 87–93. http://dx.doi.org/10.1016/j.mib.2008.02.007, (URL ⟨http://www.sciencedirect.com/science/article/pii/S1369527408000155⟩).
Görke, B., Stülke, J., 2008. Carbon catabolite repression in bacteria: many ways to make the most out of nutrients. Nat. Rev. Microbiol 6 (8), 613–624. http://dx.doi.org/10.1038/nrmicro1932.
Govern, C., ten Wolde, P., 2014. Energy dissipation and noise correlations in biochemical sensing. Phys. Rev. Lett. 113 (25), 258102. http://dx.doi.org/10.1103/PhysRevLett.113.258102.
Govern, C., ten Wolde, P., 2014. Optimal resource allocation in cellular sensing systems. In: Proceedings of the National Academy of Science USA, 111 (49), pp. 17486–17491. http://dx.doi.org/10.1073/pnas.1411524111
Inada, T., Kimata, K., Aiba, H., 1996. Mechanism responsible for glucose-lactose diauxie in Escherichia coli: challenge to the cAMP model. Genes Cells 1 (3), 293–301.
King, O., Masel, J., 2007. The evolution of bet-hedging adaptations to rare scenarios. Theor. Popul. Biol. 72 (4), 560–575. http://dx.doi.org/10.1016/j.tpb.2007.08.006.
Koirala, S., Wang, X., Rao, C., 2015. Reciprocal regulation of l-arabinose and d-xylose metabolism in Escherichia coli. J. Bacteriol. 198 (3), 386–393. http://dx.doi.org/10.1128/JB.00709-15.
Kompala, D., Ramkrishna, D., Jansen, N., Tsao, G., 1986. Investigation of bacterial growth on mixed substrates: experimental evaluation of cybernetic models. Biotechnol. Bioeng. 28 (7), 1044–1055. http://dx.doi.org/10.1002/bit.260280715.
Kotte, O., Volkmer, B., Radzikowski, J., Heinemann, M., 2014. Phenotypic bistability in Escherichia coli's central carbon metabolism. Mol. Syst. Biol. 10, 736.
Kremling, A., Kremling, S., Bettenbrock, K., 2009. Catabolite repression in Escherichia coli- a comparison of modelling approaches. FEBS J. 276 (2), 594–602. http://dx.doi.org/10.1111/j.1742-4658.2008.06810.x.
Kwiatkowska, M., Norman, G., Parker, D., 2001. PRISM: Probabilistic symbolic model checker, In: Kemper, P., (Ed.), Proceedings Tools Session of Aachen 2001 International Multiconference on Measurement, Modelling and Evaluation of Computer-Communication Systems, pp. 7–12, available as Technical Report 760/2001, University of Dortmund.
Lan, G., Sartori, P., Neumann, S., Sourjik, V., Tu, Y., 2012. The energy-speed-accuracy trade-off in sensory adaptation. Nat. Phys. 8 (5), 422–428.
Lendenmann, U., Egli, T., 1995. Is Escherichia coli growing in glucose-limited chemostat culture able to utilize other sugars without lag? Microbiology 141, 71–78, (Pt 1).
Lendenmann, U., Snozzi, M., Egli, T., 1996. Kinetics of the simultaneous utilization of sugar mixtures by Escherichia coli in continuous culture. Appl. Environ. Microbiol. 62 (5), 1493–1499, (http://arxiv.org/abs/http://aem.asm.org/content/62/5/1493.full.pdf+html URL ⟨http://aem.asm.org/content/62/5/1493.abstract⟩).
Müller, J., Hense, B.A., Fuchs, T.M., Utz, M., Pötzsche, C., 2013. Bet-hedging in stochastically switching environments. J. Theor. Biol. 336, 144–157. http://dx.doi.org/10.1016/j.jtbi.2013.07.017.
Mehta, P., Schwab, D., 2012. Energetic costs of cellular computation. In: Proceedings of the National Academy of Science USA, 109 (44), pp. 17978–17982. http://dx.doi.org/10.1073/pnas.1207814109
Mettetal, J., Muzzey, D., Pedraza, J., Ozbudak, E., van Oudenaarden A., 2006. Predicting stochastic gene expression dynamics in single cells. In: Proceedings of the National Academy of Science USA, 103 (19), pp. 7304–7309. http://dx.doi.org/10.1073/pnas.0509874103
Monod, J., 1949. The growth of bacterial cultures. Annu. Rev. Microbiol. 3, (371–349).
Narang, A., Pilyugin, S., 2007. Bacterial gene regulation in diauxic and non-diauxic growth. J. Theor. Biol. 244 (2), 326–348. http://dx.doi.org/10.1016/j.jtbi.2006.08.007.
Narang, A., 2006. Comparative analysis of some models of gene regulation in mixed-substrate microbial growth. J. Theor. Biol. 242 (2), 489–501.
New, A., Cerulus, B., Govers, S., Perez-Samper, G., Zhu, B., Boogmans, S., Xavier, J., Verstrepen, K., 2014. Different levels of catabolite repression optimize growth in stable and variable environments. PLoS Biol. 12 (1), e1001764. http://dx.doi.org/10.1371/journal.pbio.1001764.
Schuetz, R., Zamboni, N., Zampieri, M., Heinemann, M., Sauer, U., 2012. Multidimensional optimality of microbial metabolism. Science 336 (6081), 601–604. http://dx.doi.org/10.1126/science.1216882.
Solopova, A., van Gestel, J., Weissing, F.J., Bachmann, H., Teusink, B., Kok, J., Kuipers, O.P., 2014. Bet-hedging during bacterial diauxic shift. In: Proceedings of the National Academy of Sciences, 111 (20), pp. 7427–7432. http://dx.doi.org/10.1073/pnas.1320063111
Stülke, J., Hillen, W., 1999. Carbon catabolite repression in bacteria. Curr. Opin. Microbiol. 2 (2), 195–201. http://dx.doi.org/10.1016/S1369-5274(99)80034-4, (URL ⟨http://www.sciencedirect.com/science/article/pii/S1369527499800344⟩).
Venturelli, O., Zuleta, I., Murray, R., El-Samad, H., 2015. Population diversification in a yeast metabolic program promotes anticipation of environmental shifts. PLoS Biol. 13 (1), e1002042. http://dx.doi.org/10.1371/journal.pbio.1002042.
Wang, J., Atolia, E., Hua, B., Savir, Y., Escalante-Chong, R., Springer, M., 2015. Natural variation in preparation for nutrient depletion reveals a cost-benefit tradeoff. PLoS Biol. 13 (1), e1002041. http://dx.doi.org/10.1371/journal.pbio.1002041.
Zabet, N., Chu, D., 2010. Computational limits to binary genes. J. R. Soc. Interface 7 (47), 945–954. http://dx.doi.org/10.1098/rsif.2009.0474.